JOURNAL OF THERMOPHYSICS AND HEAT TRANSFER
Vol. 8, No. 1, Jan.–March 1994

Startup Performance of a Liquid-Metal Heat Pipe in Near-Vacuum and Gas-Loaded Modes

R. Ponnappan*
Universal Energy Systems, Inc., Dayton, Ohio 45432
and
W. S. Chang†
Wright Laboratory, Wright-Patterson Air Force Base, Ohio 45433

Understanding the startup behavior of a heat pipe from frozen state has received a lot of attention in recent years. In liquid-metal heat pipes, a calculated amount of inert gas is filled as one of the safest means to start them from a frozen state. In the present study, an arterial-type sodium heat pipe with a long transport section has been tested for startup performance in both vacuum and gas-filled modes. A comparison was necessary to contrast the relative merits of gas-filled mode startup from the conventional vacuum mode. The 2-m-long heat pipe with 2.0-Torr argon started very smoothly from frozen state for suddenly applied evaporator loads up to 1.1 kW. Only less than 5% of the total length remained as inactive condenser due to the gas loading. The same heat pipe in the vacuum mode had large temperature spikes at the evaporator and heater during the frozen startup indicating a rough startup behavior.

Nomenclature

L = length, m
L_g = noncondensible gas-blocked length of the pipe, m
L_p = total length of the heat pipe, m
P_i = initial gas charge pressure, N/m^2
P_v = vapor pressure of working fluid, N/m^2
Q_i, Q_{in} = evaporator heat input (electric heater), W
Q_0, Q_{out} = condenser heat output (calorimeter), W
T = operating temperature of heat pipe, K
T_c = room temperature at the time of gas loading, K
T_H = hot zone temperature, K
$\bar{T}_H$ = average hot zone temperature, K
T_S = sink temperature, K
ΔT_{EA} = evaporator end (thermocouple no. 3) to adiabatic (thermocouple no. 7) temperature difference, K
ε = emissivity of condenser external surface

Subscripts
A = adiabatic
C = condenser
E = evaporator
R = reservoir

Introduction

LIQUID-METAL heat pipes (LMHP) using potassium, sodium, and lithium as working fluids have potential application in space power systems such as SP-100, space station, and a variety of military spacecraft. Also, gas-loaded LMHPs are used in terrestrial applications such as isothermal blackbody standards for sensor calibration and semiconductor single crystal processing.[1,2] In all these applications of the LMHPs, some of the important performance criteria to be investigated are startup, shutdown, isothermality, and active condenser length regulation. Noncondensible gas (NCG) filling converts a conventional heat pipe into a variable conductance heat pipe (VCHP). Low temperature VCHPs have been extensively researched in the past and they are used in thermal control application of low power communication satellites. However, only a limited number of research publications are available in the high-temperature VCHPs. Also, it is believed in certain sections of the heat pipe research community that LMHPs do not have any startup problems and any attempt to gas-load a LMHP would adversely affect the priming of arterial type heat pipes.[3] In order to understand these problems closely, a 2-m stainless steel—sodium, argon filled, grooved artery heat pipe was designed, fabricated, and tested. Experimental results showed successful startup and performance.[4–6]

It is extremely difficult to fabricate a perfectly gas-free heat pipe in actuality. Because heat pipes are usually long and slender tubes, evacuating them to ultrahigh vacuum levels (10^{-8} Torr or better) before filling with working fluids is impossible. For a typical heat pipe 2-m long, 2.22-cm vapor core diameter, if the fill tube end is at 10^{-6} Torr, the closed end will be at 10^{-4} Torr, assuming reasonable outgassing rate for the pipe and pumping capacity for the vacuum pump. Hence, there is always a small quantity of residual gas left inside the pipe. The quantity of residual gas (ideal gas) at 10^{-4} Torr and 300 K is 13.78×10^{-10} gm for the heat pipe mentioned above. In addition to the residual gas, there are other sources of gas contributing to the total NCG that may be present within the heat pipe. For example, the internal surfaces of the pipe and wick structure may degas at high operating temperatures due to minute impurities and absorbed gases which are released on heating.[7] If a LMHP is operating in a moist environment, there is the likelihood of hydrogen permeation into the pipe.[3] Hence, in a practical sense, truly vacuum mode heat pipe is nonexistent. On the other hand, gas loaded on purpose or already present as residual gas, if it contributes to the easy and rapid startup from frozen state and problem-free shutdown, may lead to a class of heat pipe that can be exploited for practical applications.

Presented as Paper 90-1755 at the AIAA/ASME 5th Joint Thermophysics and Heat Transfer Conference, Seattle, WA, June 18–20, 1990; received July 17, 1992; revision received May 12, 1993; accepted for publication May 13, 1993. Copyright © 1993 by R. Ponnappan and W. S. Chang. Published by the American Institute of Aeronautics and Astronautics, Inc., with permission.

*Principal Research Scientist, Scientific and Engineering Services Division. Senior Member AIAA.
†Research Scientist, Aero Propulsion and Power Directorate. Member AIAA.

The objective of the present study is to obtain the comparative performances of a LMHP in vacuum and gas-filled modes, and to verify the smooth and rapid startup of the gas-filled mode from frozen state. The performance characteristics including the frozen state startup of the near-vacuum mode and gas-loaded mode of a particular LMHP are presented. Also, it is shown that gas loading could be predetermined in LMHPs such that the inactive condenser length is kept very small and no gas reservoir is required.

Theoretical Consideration

The operating temperature of the heat pipe and the gas charge pressure will vary depending upon the working fluid used. The gas-blocked length of the condenser can be designed to vary from full length at startup to less than 5% of the full length based on the working fluid and the initial gas charge pressure.

For a cylindrical heat pipe of uniform vapor core cross section, the ratio of gas-blocked length to total pipe length is approximately given in terms of the pressure ratio as in Eq. (1)[5,8]:

$$\frac{L_g}{L_p} = \frac{P_t(T_c)}{P_v(T)} \tag{1}$$

In deriving Eq. (1), it has been assumed that 1) the noncondensible gas behaves as an ideal gas at the heat pipe operating temperature and pressure; 2) a narrow diffusion region separates the hot vapor zone and the cold gas zone under steady state; 3) axial conduction along the wall and wick is neglected; and 4) the gas is compressed to the pressure of the working fluid vapor at the hot zone temperature.

Figure 1 shows the graphical results of Eq. (1) for sodium. The fraction of the heat pipe length blocked by NCG is plotted as a function of temperature for various possible initial gas charge pressures (0.005–100 Torr). The recommended nominal operating temperature based on the optimum liquid transport factor for sodium is 1000 K. The operating temperature range for sodium is normally ±300 K from this nominal temperature. The initial gas charge pressure range of 0.005–100 Torr is chosen based on this temperature range. It is to be noted that a gas-loaded LMHP does not startup until the vapor pressure of the working fluid equals or exceeds the value of the initial gas charge pressure. It can be seen in Fig. 1, for an initial gas charge pressure of 2.0 Torr, that the gas-blocked length at the nominal operating temperature is less than 5% of the total length.

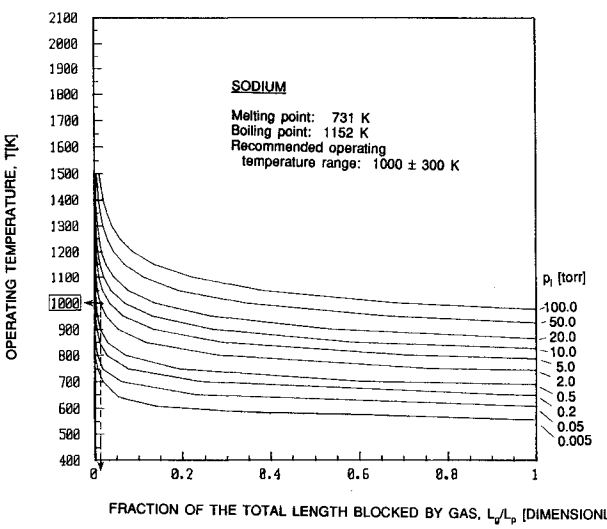

Fig. 1 Gas-blocked length as a function of initial gas charge pressure for sodium LMHP.

Experimental Work

Test Article Description

The experimental LMHP was made of stainless-steel material and filled with sodium as the working fluid. The wick structure was of the "double wall artery" design with only one transport artery groove channel. The evaporator and condenser sections had identical grooved inner tube and screen tube wick construction. The cross-sectional and longitudinal sectional views of the heat pipe are shown in Figs. 2a and 2b, respectively. The total length was 2.03 m and the diameter was 2.22 cm. Each of the 24 evaporator and condenser grooves was 0.79-mm wide and 1.40-mm deep, while the single adiabatic groove was 2.38-mm square. The adiabatic artery groove was made bigger in order to reduce fluid frictional loss. It was sized such that the artery could prime from smaller condenser groove without any problem for the range of design transport capacity. The evaporator, transport, and condenser lengths were 33, 79, and 91 cm, respectively, and the effective length was 1.388 m. The central line axis along the groove bottom in the transport section was collinear with the corresponding evaporator and condenser grooves in alignment. The 12.5-cm-long, 1.89-cm-diam, 40- × 40-cm^{-1}, 75.25% porous reservoir wick was in capillary contact with the 40- × 40-cm^{-1}, 62.9% porous evaporator screen wick. The pipe was loaded with 92.04 g of pure sodium calculated for optimum fill at 1000 K operation. A bellows-type high temperature all metal valve, rated good for 649°C at 1700 kPa, enabled the processing of sodium or inert gas to or from the pipe. A

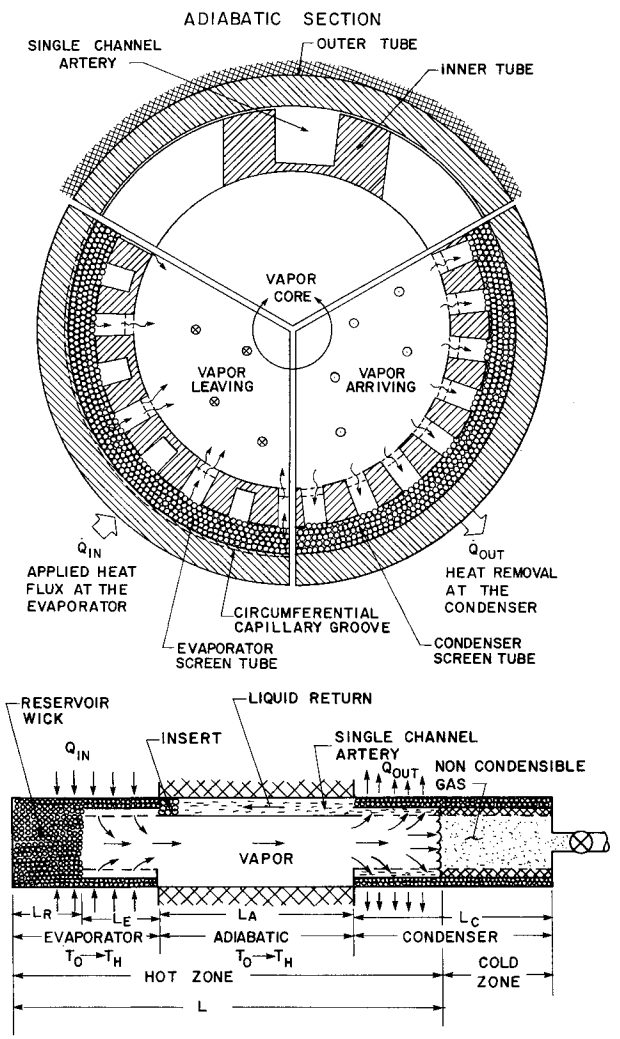

Fig. 2 Geometry of the test article sodium LMHP: a) cross-sectional view and b) longitudinal section view.

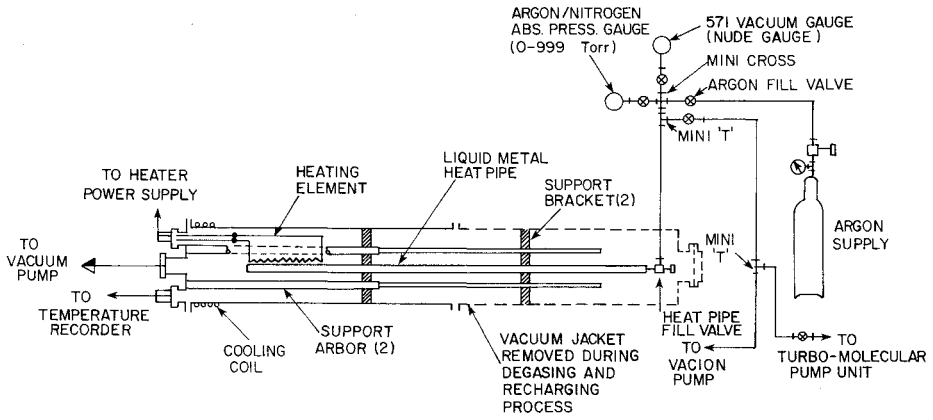

Fig. 3 Noncondensible gas charging and pressure measurement schematic diagram.

comprehensive description of the design and processing details can be found in Ref. 5.

Test Setup

The LMHP was instrumented with electrical resistance heaters for the evaporator and trace heating, and chromel-alumel thermocouples for external wall temperature measurement. The main heater was made of pyrolytic graphite strips coated (CVD) on boron nitride substrate and covered with the same material. The thin walled custom designed tubular heater was capable of operation up to 2000°C in vacuum. The heater was radiatively coupled to the heat pipe in order to reduce the evaporator thermal mass. High-temperature ceramic insulator and multiple layers of polished stainless-steel radiation shields provided heat insulation to the heat pipe which was mounted concentrically within a 20-cm-diam, 230-cm-long vacuum chamber. Cooling water circulating in coils wrapped around the chamber provided the heat sink and calorimeter for the test. The chamber was pumped down to 10^{-6} Torr or better for eliminating convective losses and corrosion of the LMHP. The frame holding the chamber was mounted on a fulcrum support to enable tilting of the heat pipe for force priming in case of a dryout.

A plumbing arrangement as shown in the schematic of Fig. 3 was used whenever the gas pressure inside the heat pipe was to be measured or changed. The vacuum system was capable of 10^{-8} Torr holding-vacuum, and the argon/nitrogen pressure gauge could measure absolute pressure in $\pm 0.5\%$ increments up to 999 Torr.

Test Procedure

At the beginning of the present round of tests, the LMHP was reprocessed to make up for the sodium lost. About 25% of the inventory was collected in a glass measuring jar and weighed during an earlier gas venting operation performed in hot (500°C) and vacuum conditions. As the refilling process was done under high-vacuum conditions, the pipe was considered to be in near-vacuum mode. Transient and steady-state test were conducted in this mode in horizontal position with the adiabatic artery at the 3 o'clock orientation. Startup tests from frozen state were usually started in the beginning of the day when the pipe had cooled down to room temperature. In a typical test run, a desired constant power input was applied to the evaporator in one step, and the temperatures along the length of the pipe were recorded at intervals of one minute for nearly 3 h. High-temperature alarm limits were set on the heater and evaporator thermocouples to cut off the heater power. Transient tests were usually followed by steady-state tests. The condenser shutters were locked in fully closed position. This arrangement prevented the condenser from quenching and at the same time, allowing sufficient radiation to pass through. At steady-state, power input, axial temperatures, cooling water inlet, outlet temperatures, and flow rate were recorded.

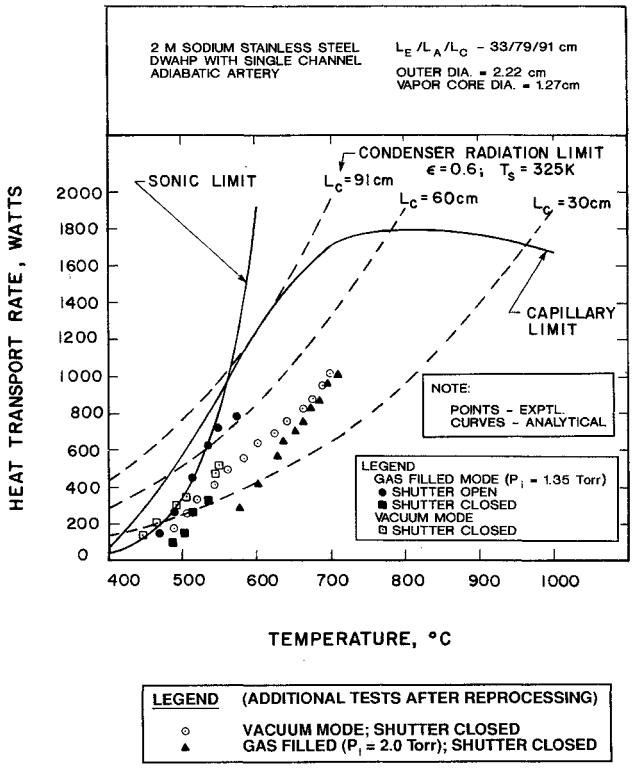

Fig. 4 Predicted and experimental performances (Q_0 vs T_H).

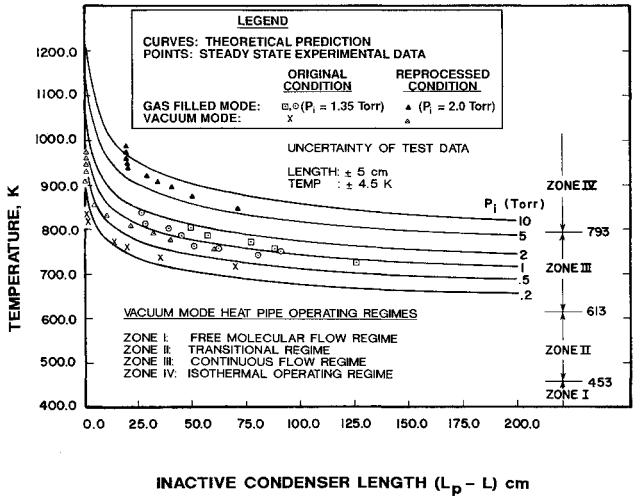

Fig. 5 Steady-state inactive condenser length for different test conditions.

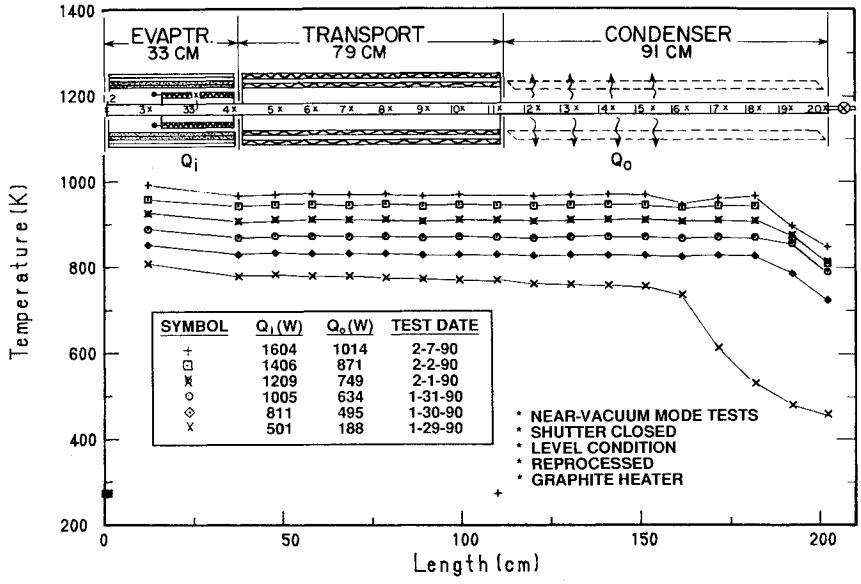

Fig. 6 Steady-state axial temperature profile (vacuum mode).

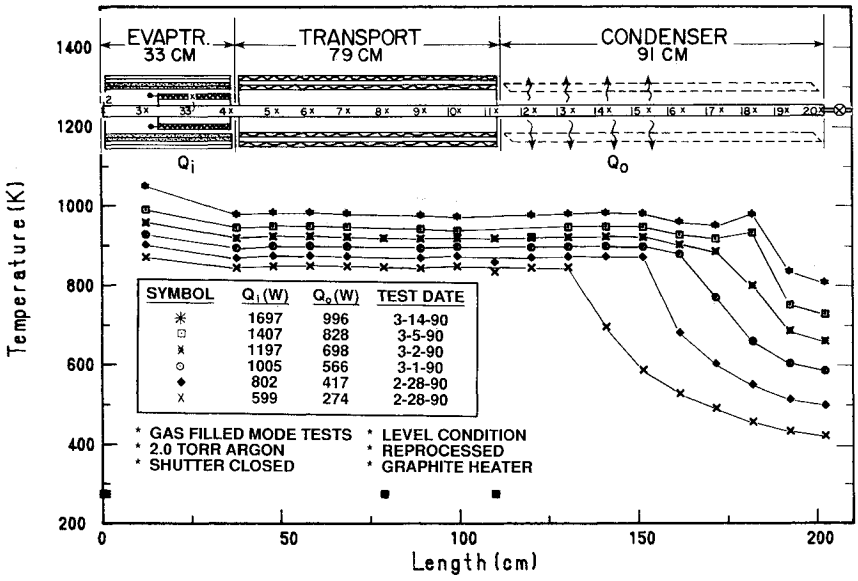

Fig. 7 Steady-state axial temperature profile (gas-filled mode).

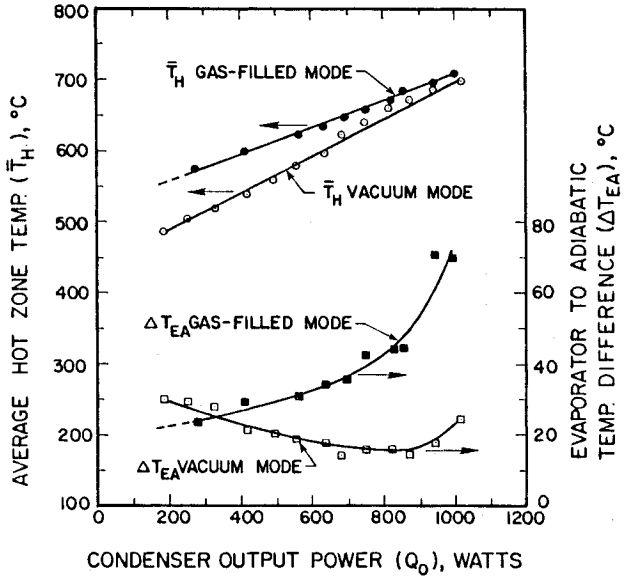

Fig. 8 Average hot zone temperature and temperature difference.

After vacuum mode tests, the LMHP was filled with 2.0 Torr of argon using the rig shown in Fig. 3. Then the functional tests were repeated in the gas-filled mode in the same manner described above.

Results and Discussions

The accuracies of temperature, power, and flow measurements were reasonable and the repeatability of test results were good. The output power measured through the calorimetric data was within 5% of the electric power input measured. Mostly, the vacuum and gas-filled mode startup test results of the reprocessed pipe are compared and discussed here. In addition, the transport capacity and inactive condenser length data for all the tests done so far on this LMHP are presented.

Transport Capacity

The experimental transport capacity data are plotted along with the theoretically predicted sonic and capillary limit curves in Fig. 4. The experimental points correspond to the average hot zone temperature $\bar{T}_H$, and the condenser radiated power Q_0. It may be noted that with the graphite heater the LMHP could be run at 1000 K, transporting nearly 1000 W. The data

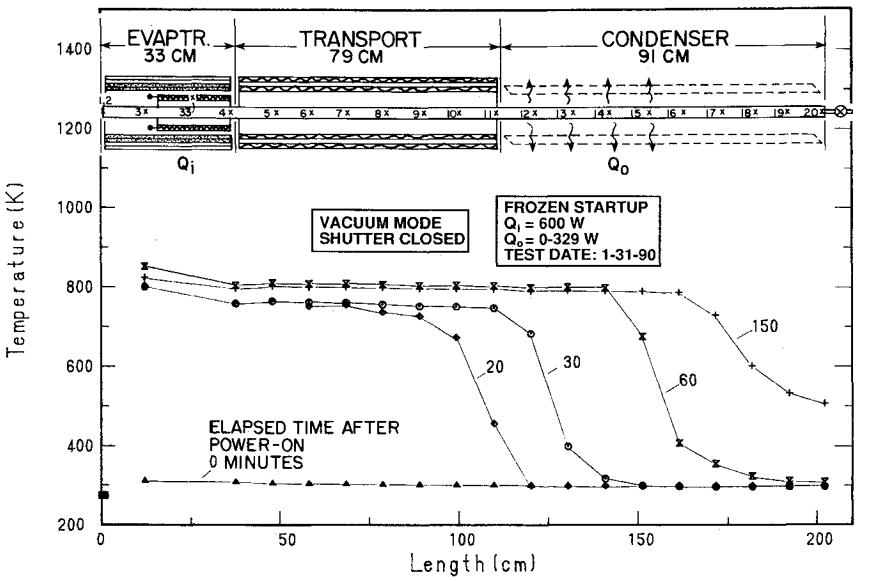

Fig. 9 Axial temperature profile at specified time from 0–150 min after power input (Q_i = 600 W; vacuum mode).

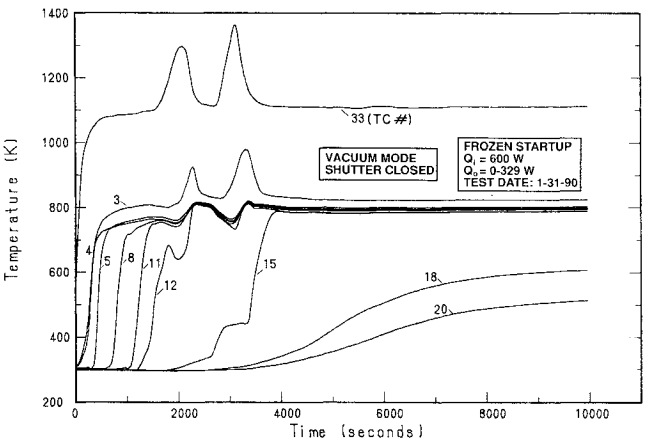

Fig. 10 Transient temperature profile at specified axial locations (Q_i = 600 W; vacuum mode).

points lie away from the sonic and capillary limit curves due to the closed shutter condition which made the pipe run at higher temperatures than normal. The average operating temperature of the hot zone could have been reduced by opening the condenser shutter. The shutter opening mechanism was broken during these tests. The pipe was not operated near the designed maximum transport limit of 1800 W for safety reasons. The heater was running at 1250°C when the average hot zone was near 800°C. As the temperature of the pipe went up, it became riskier to run the test; more thermocouples broke and the heater got closer to meltdown. Therefore, a 1000 K operating temperature limit was set and adhered to.

The maximum transport capacity attained in both vacuum and gas modes were the same. At low transport rates (<500 W) the pipe operated at lower temperatures (about 50–100 K lower) in vacuum mode compared to the gas mode for identical test conditions, due to the effective condenser length variation.

Inactive Condenser Length

Figure 5 shows the inactive condenser length as a function of the operating temperature for various test conditions. As can be seen from the figure, in vacuum mode tests, there is no inactive condenser with sufficient power input to the pipe. At low power levels only a fraction of the condenser is needed to dissipate the heat load, and therefore these points do not represent gas slugged length. In the case of gas-loaded mode, all the data points above 935 K show 18 cm of gas-blocked condenser. The 2.0-Torr gas mode experimental data lie along the 5–10-Torr theoretical curves. The reason for the lateral shift is attributed to the heating of the inactive condenser (gas-blocked length) by the reradiation from the closed condenser shutters. This experimental setting happens to be in violation of the assumption that the cold zone is at the sink temperature as described in Eq. (1). If a correction is applied to offset the reheating effects on the gas, it can be shown that the 2.0-Torr gas data will match with the theoretical curve. The axial temperature profiles of the gas mode are explained in the next section and should be referred to for better understanding.

Axial Temperature Profile

The steady-state axial temperature profiles of the LMHP for vacuum and gas modes are given in Figs. 6 and 7, respectively. The test conditions are indicated therein. The thermocouples 1 and 2 were damaged. In both modes, the profiles corresponding to input power range of 600–1600 W are plotted. The condenser power output as measured in the calorimeter is listed under Q_0. The heater temperature varied from 1021 K for the lowest Q_i to 1486 K for the highest Q_i, while the hot zone operating temperature varied from 800 to 1000 K in both modes.

As expected, the condenser section profiles are distinctly different for vacuum and gas modes, while the evaporator and transport profiles are similar. In the vacuum mode, the pipe is near-isothermal from end-to-end for Q_i greater than 800 W. A small drop in condenser-end temperature is indicative of the presence of trace amounts of noncondensible gas or excess fluid. In the gas mode, the gas-blocked section is closely noticeable at all power levels. In normal circumstances, the condenser-end temperature should be close to the cold sink temperature. However, here it is seen to increase with the power input. The reason for this behavior is attributed to the closed condenser shutter which reradiated and heated the condenser end. The profiles for a partially open shutter condition where the end temperatures were near 400 K are reported in Ref. 4.

Temperature Difference

$\bar{T}_H$ and ΔT_{EA} for both modes of the LMHP are plotted in Fig. 8. The points in this graph represent experimental data, while the lines represent intuitive curve fit for the data. $\bar{T}_H$ for both modes vary linearly with transported power, whereas ΔT_{EA} data vary nonlinearly. For the gas mode, the range of

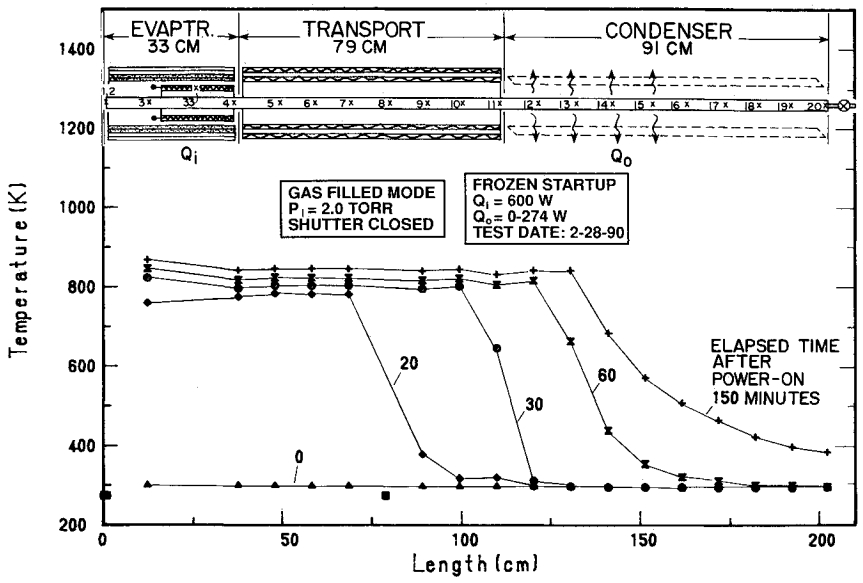

Fig. 11 Axial temperature profile at specified time, from 0–150 min after power input (Q_i = 600 W; gas-filled mode).

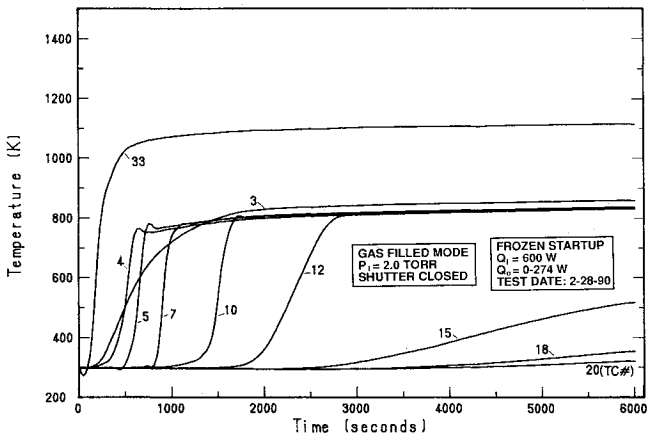

Fig. 12 Transient temperature profile at specified axial locations (Q_i = 600 W; gas-filled mode).

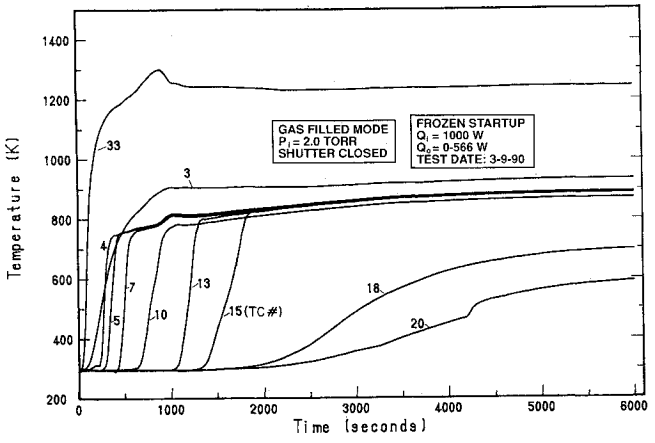

Fig. 14 Transient temperature profile at specified axial locations (Q_i = 1000 W; gas-filled mode).

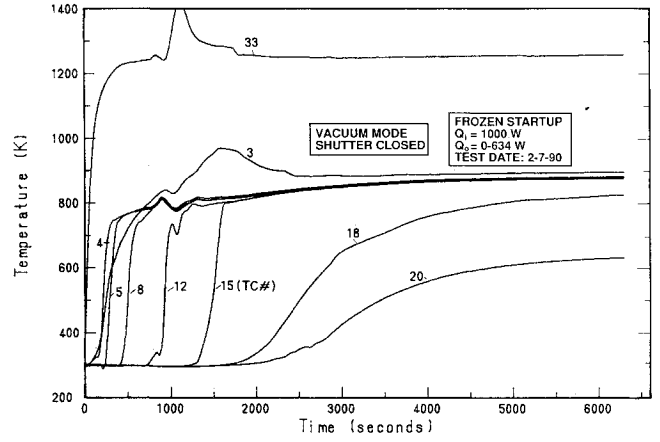

Fig. 13 Transient temperature profile at specified axial locations (Q_i = 1000 W; vacuum mode).

$\bar{T}_H$ is narrower than that for the vacuum mode, and this is the expected behavior for a VCHP known for closer temperature control. Comparison of the ΔT_{EA} behavior for the two modes is interesting to observe. The vacuum mode ΔT_{EA} curve is typical of the lean evaporator behavior, characteristic of the double wall wick, wherein the temperature difference decreases with increase in power.[9] On the other hand, in the gas mode the ΔT_{EA} increases with power, which means that the liquid superheat at the evaporator wall is increasing with temperature. The latter behavior is similar to the classical Rohsenow and Bergles theory of nucleate boiling phenomenon in the presence of noncondensible gas as explained in Ref. 10. The high ΔT_{EA} at higher Q_0 in the gas mode is symptomatic of an impending evaporator dryout. The trend of the ΔT_{EA} curve indicates that a gas-loaded arterial heat pipe might fail at lower power levels than a similar conventional pipe due to artery priming crisis. However, this concern could be remedied by artery redesign rather than abandoning the idea of gas-loaded mode startup. The influence of the gas on the evaporator dryout is a gray area which needs further study.

Frozen Startup Behavior

Successful Startup

The LMHP was tested under identical test configuration and test procedure for both vacuum and gas modes. The vacuum mode tests preceded the gas mode tests. The startup tests from a frozen state were started when the pipe was at room temperature (20°C) by suddenly applying the desired power to the evaporator heater and maintaining it at the same level throughout the test duration (about 2–3 h). The transient behavior of the pipe was monitored by recording the temperature at all the axial locations for every minute.

The results are presented in the form of axial and transient temperature profiles. Even though tests were done at 100-W

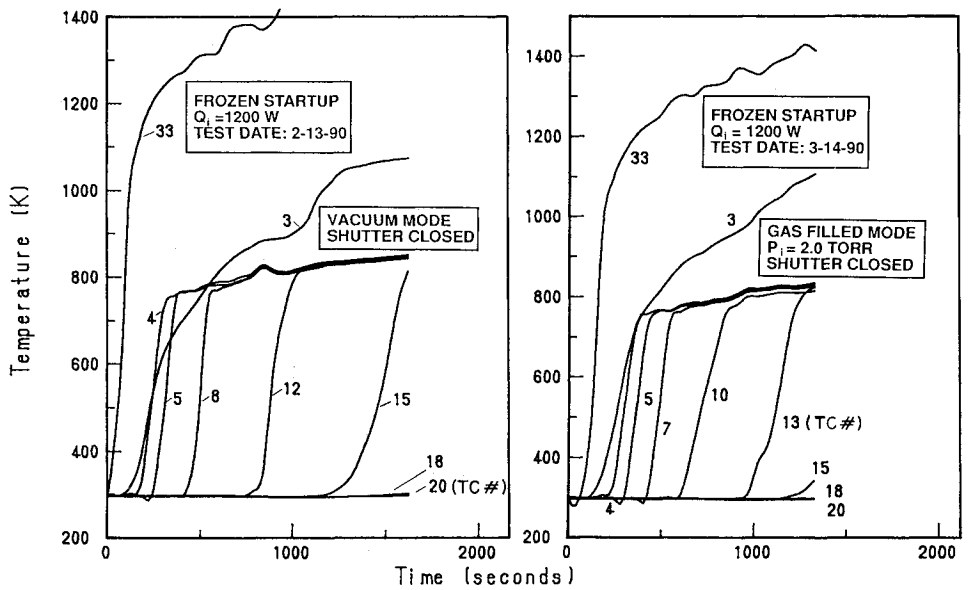

Fig. 15 Evaporator and heater temperature "run-away" condition during 1200-W input (vacuum and gas-filled modes).

power increments, from 300 to 1200 W, only a couple of the representative graphs are presented here. Figures 9 and 10 show the 600-W vacuum mode plots in the form of axial temperature profiles at specified times, and transient temperature profiles at specified axial locations, respectively. Figures 11 and 12 show the corresponding 600-W gas-filled mode behavior. As seen from Figs. 9 and 11, in 20 min the hot vapor front has propagated to the condenser region in vacuum mode, while the front has crossed only the midsection of the adiabatic in gas mode. At 150 min, the hot front has moved to 170 cm in vacuum mode, while it has moved to 130 cm in gas mode. It is clear from Fig. 10 that the startup was not smooth in vacuum mode since thermocouple (T.C.) no. 33 (heater) experienced sudden high-temperature spikes 2000 s after power-on. This is a temporary crisis of wall superheat at the evaporator end, if not self-corrected, could lead to evaporator burnout. In contrast, the gas mode startup was smooth (Fig. 12) since T.C. nos. 3 and 33 did not experience any surge.

Similarly, the results of the frozen startup tests with 1000-W input for vacuum and gas modes are presented in Figs. 13 and 14, showing the transient temperature profiles. As in the 600-W case, the startup in the vacuum mode was rough, while that in the gas mode was smooth. However, a small hump is noticeable in Fig. 14 for T.C. no. 33 at 900 s, indicating a temporary crisis. For the 1100-W input case (plot not shown), T.C. no. 3 also showed a 100 K spike which forewarned startup trouble for the gas-filled mode. This indicates that even with gas loading, the startup could be rough if the initial charge pressure is not adequate enough. Also, it shows that we have reached the heat input step maximum limit for the P_i chosen.

Other important information obtained from Figs. 10, 12, 13, and 14 is the comparison of the startup time for both modes. The heat pipe is supposed to have started successfully if the hot front has crossed T.C. no. 11 (adiabatic region). As seen from these figures, the near-vacuum mode startup times are shorter than those for the gas mode, which is in conformity with the diffusion controlled startup theory explained in Ref. 4. According to this theory, startup time increases with an increase in initial gas charge pressure.

Startup Failure

The input power was increased to 1200 W after successful startup with 1100 W in gas mode. But this time the temperatures of T.C. nos. 3 and 33 kept rising until the alarm limits were reached. This test was repeated several times with the same outcome. Hence, it was concluded that 1100 W was the maximum limit that this LMHP could successfully be started from a frozen state. Figure 15 shows the startup failure in both modes for 1200-W input.

Conclusions

Based on the experimental investigations performed on a 2-m-long sodium-stainless steel double wall artery heat pipe in vacuum and gas-filled modes, the following conclusions were reached:

1) The steady-state performances were verifiable up to 1014 W of condenser transport which was 56% of the designed transport capacity (1800 W) for the single artery LMHP. Tests could not be continued beyond this level without surpassing the safe operating limits of 1000 K for the heat pipe and 1550 K for the heater.

2) A true vacuum mode of the LMHP was not attainable due to the limitations of the heat pipe processing facility. However, a near-vacuum mode was attainable to compare and contrast with the gas-filled mode.

3) As predicted, the steady-state gas-blocked inactive condenser length was within 5% of the total heat pipe length after correcting for the cold zone temperature for the 2.0-Torr argon-filled mode.

4) In the vacuum mode, the pipe was operating near-isothermal from end-to-end for 800–1000 K, and transporting 495–1014 W. In the gas mode, the hot zone remained isothermal within a ΔT of 10 K.

5) For the same transport capacity variation of 500–1000 W, the pipe average hot zone operating temperature varied 130 K in vacuum mode and 90 K in gas mode, which confirms better temperature control for noncondensible gas filled heat pipes. This is the expected behavior just as in VCHP.

6) The evaporator to adiabatic temperature difference dropped with an increase in transported power for vacuum mode, while it increased for the gas mode. The vacuum mode characterized the lean evaporator behavior of the double wall wick, while the gas mode characterized the nucleate boiling phenomenon in an inert gas environment.

7) The frozen startup tests were smooth and successful in the gas-filled mode for heat inputs up to 1000 W (Q_i), giving a transport of 640 W (Q_0) which is 35.5% of the designed transport capacity. For the vacuum mode, the frozen startups were rough and successful up to the same transport. However, the LMHP could not be started from frozen state for power inputs ≥1200 W in both modes.

Acknowledgments

This research was performed under the auspices of the U.S. Air Force at the Aero Propulsion and Power Directorate of

the Wright Laboratory and the Strategic Defense Initiative Organization. The technical services by J. Tennant and M. Ryan are appreciated.

References

[1]Brost, O., Groll, M., and Mack, H., "Development of a High Temperature Furnace with Variable Conductance Heat Pipe," *Proceedings of the 6th International Heat Pipe Conference*, Grenoble, France, May 25–29, 1987, pp. 697–702.

[2]Tolubinsky, V. I., Shevchek, E. N., and Kudritskaya, L. V., "Study of Vapor-Gas Front Temperature Characteristics in Sodium Coaxial Heat Pipes," *Proceedings of the 6th International Heat Pipe Conference*, Grenoble, France, May 25–29, 1987, pp. 326–329.

[3]Merrigan, M., private communication, Los Alamos National Lab., Los Alamos, NM.

[4]Ponnappan, R., Boehman, L. I., and Mahefkey, E. T., "Diffusion Controlled Startup of a Gas-Loaded Liquid Metal Heat Pipe," *Journal of Thermophysics and Heat Transfer*, Vol. 4, No. 3, 1990, pp. 332–340.

[5]Ponnappan, R., "Studies on the Startup Transients and Performance of a Gas Loaded Sodium Heat Pipe," WRDC-TR-89-2046, Wright-Patterson AFB, OH, June 1989.

[6]Ponnappan, R., Boehman, L. I., and Mahefkey, E. T., "Transient Characteristics of a Gas Loaded Liquid Metal Heat Pipe with a Long Adiabatic Section," *Space Power*, Vol. 8, No. 4, 1989, pp. 477–492.

[7]Ranken, W. A., "Space Reactors," Los Alamos National Lab., Progress Rept. LA-9146-PR, Los Alamos, NM, April–June 1981, pp. 17–22.

[8]Ponnappan, R., Beam, J. E., and Mahefkey, E. T., "A Liquid Metal Variable Conductance Heat Pipe for Space Radiators," 7th Symposium on Space Nuclear Power Systems, Albuquerque, NM, Jan. 7–11, 1990.

[9]Ponnappan, R., and Mahefkey, E. T., "Development of a Double-Wall Artery High-Capacity Heat Pipe," *Spacecraft Thermal Control, Design and Operation*, edited by P. E. Bauer and H. E. Collicott, Vol. 86, Progress in Astronautics and Aeronautics, AIAA, New York, 1983, pp. 202–221.

[10]Marcus, B. D., "Theory and Design of Variable Conductance Heat Pipes," NASA CR-2018, April 1972.